Planta (1989) 179:516–529

Planta

The generation and consolidation of a radial array of cortical microtubules in developing guard cells of *Allium cepa* L.

J. Marc*, Y. Mineyuki, and B.A. Palevitz**
Department of Botany, University of Georgia, Athens, GA 30602, USA

Abstract. The initiation and development of a radial array of microtubules (MTs) in guard cells of *A. cepa* was studied using immunofluorescence microscopy of tubulin in isolated epidermal layers. Soon after the completion of cytokinesis, MTs originate in the cortex adjacent to a central strip of the new, anticlinally oriented ventral wall separating the two guard cells. Cortical MTs extend from the mid-region of the central strip toward the cell edge where the ventral wall joins the inner periclinal wall. They then spread in a fan-like formation along the periclinal wall and gradually extend along the lateral and end walls as well. Many MTs criss-cross at various angles as they arc past the edge formed by the junction of the ventral and periclinal walls, but they do not terminate there, indicating that, contrary to previous reports, the edge is not involved in MT initiation. Instead, the mid-region of the central strip appears to function as a planar MT-organizing zone. Initially, MTs radiate from this zone through the inner cytoplasm as well as the cortex. During cell expansion, however, the cortical MTs increasingly predominate and consolidate into relatively thick, long bundles, while the frequency of non-cortical MTs diminishes. The apparent density of MTs per unit surface area is maintained as the cells expand and gradually flex into an elliptical shape. The guard cells eventually separate completely at the pore site. The entire process is accomplished within about 12 h.

Key words: *Allium* – Cell cortex – Cytoskeleton – Guard cell – Microtubule – Stomatal complex

* To whom correspondence should be addressed
** *Present address:* Botanical Institute, Hiroshima University, Hiroshima, Japan

Abbreviations: DIC = differential interference contrast; GC = guard cell; MT = microtubule

Introduction

Stomatal guard cells (GCs) provide not only a classical example of the correlation between cell structure and function, but also pose intriguing questions regarding mechanisms that control cell morphogenesis. At an early stage, cell-wall microfibrils are deposited in distinctive orientations and distributions (Palevitz and Hepler 1976; Doohan and Palevitz 1980; Hepler 1981; Mishkind et al. 1981; Palevitz 1981a, 1982). The role of cortical microtubules (MTs), which are typically co-aligned with the wall microfibrils (see also Giddings and Staehelin 1988), in regulating these wall characteristics has been confirmed by studies with anti-MT drugs (Palevitz and Hepler 1976; Galatis 1982). Because cell-wall properties are crucial in stomatal action (Raschke 1979), the spatial organization of MTs is thus a key factor in the determination of normal GC function.

Descriptions of MT organization are available in electron-microscope studies of taxonomically diverse species including a moss (Sack and Paolillo 1983), ferns (Galatis et al. 1983; Busby and Gunning 1984), dicotyledons (Singh and Srivastava 1973; Galatis and Mitrakos 1980), and monocotyledons (Kaufman et al. 1970; Srivastava and Singh 1972; Palevitz and Hepler 1976; Galatis 1980; Mishkind et al. 1981; Palevitz 1981a, 1982). With the exception of modifications that occur during later stages of development in grasses, the MTs characteristically radiate from the pore site outward along the periclinal walls (see also Palevitz and Mullinax 1989), but appear to be oriented anticlinally along the ventral wall separating the two GCs. The mechanisms controlling the position and orientation of these MTs are unknown, however. It has been suggested that complexes of electron-

opaque material, vesicles and converging MTs located at the edges formed by the junction of the ventral and periclinal walls function as MT-organizing centers (Galatis 1980, 1982; Galatis et al. 1983; Busby and Gunning 1984). It is unclear, however, how such centers give rise to MTs that are oriented anticlinally (and parallel to each other) at the ventral wall, as well as those oriented at divergent angles along the periclinal walls. It is also unclear how the activity at relevant edges at the inner and the outer periclinal walls would be coordinated. That cell edges may not in fact be the location of MT initiation is indicated by the observation that similar complexes in *Phleum* GCs are located elsewhere (Palevitz 1981 b).

In the diverse species examined by electron microscopy, MTs typically aggregate at relatively high density at the central portion of the ventral wall. This raises the possibility that the common origin of the cortical MTs is a zone located centrally along the ventral wall, which then provides MTs for both the inner and the outer halves of the cell. In order to examine this possibility, it is necessary to visualize the spatial organization of MTs in much of the entire cell, and in cells at various developmental stages, a task that would be laborious using reconstructed electron-microscope images of serial sections. We have therefore taken advantage of immunofluorescence microscopy and a recently developed method for the localization of MTs in isolated surface cell layers (Marc and Hackett 1989). The method retains the orientation of cells in the layer as well as the spatial organization of MT arrays. In this report we show that in the GC of *Allium* a radial array of MTs is initiated along the mid-region of a relatively narrow central strip of the ventral wall, which apparently functions as a planar MT-organizing zone. The MTs extend past the junction with the periclinal wall and spread out with increasing distance, thus forming the characteristic radial arrangement. As shown in the accompanying paper (Marc et al. 1989), during recovery after cold- or colchicine-induced MT depolymerization, this array is regenerated from the same region.

Material and methods

Seeds of *Allium cepa* L. cv. White Portugal (Harris Moran Seed Co., Rochester, N.Y., USA) were germinated in moist vermiculite at 24° C. The terminal portions of the cotyledons of 4–6-d-old seedlings were sliced longitudinally in half and 4–5-mm-long segments above the cotyledonary hook were excised. The segments were fixed overnight with 4% paraformaldehyde and 0.2% glutaraldehyde in 50 mM 1,4-piperazinediethanesulfonic acid (Pipes) buffer containing 5 mM ethyleneglycol-bis(β-aminoethylether)-N,N,N′,N-tetraacetic acid (EGTA), 1 mM $MgSO_4$ and 1% glycerol, pH 6.8. After a brief rinse in buffer and infiltration with 20% glycerol for 10–20 min, the segments were attached to glass microslides (Carlson Scientific, Peotone, Ill., USA), the epidermal surface next to the glass, with cyanoacrylic glue (Krazy Glue, Itasca, Ill., USA). The glue was allowed to polymerize under a drop of distilled water for 10–30 min before trimming the tissue with a fine blade (Fine Science Tools, Belmont, Cal., USA), so that only a few inner cell layers covered the epidermis. The preparations were then digested for 10–20 min with a solution containing 1% Cellulase Onozuka R-10 and 1% Macerozyme R-10 (Serva Biochemicals, Westbury, N.Y., USA), 0.4 M mannitol, 5 mM ethylenediaminetetraacetic acid (EDTA), 0.1% Nonidet P-40 (Sigma Chemical Co., St. Louis, Mo., USA), 1% bovine serum albumin (BSA) (Sigma) and a mixture of protease inhibitors (1 mM phenylmethylsulfonylfluoride [PMSF], 40 μg/ml leupeptin, 25 μg/ml chymostatin, and 5 μg/ml each of antipain, aprotinin, α-2-macroglobulin and pepstatin A; all from Sigma). Following digestion the preparations were rinsed with distilled water and maintained moist during subsequent operations. Extraneous subepidermal cells were removed with a fine brush, leaving a cylindrical epidermal layer supported by the polymerized glue. Thus the epidermis is observed by viewing its inner periclinal surface (see Fig. 1).

Before processing for tubulin immunofluorescence, the preparations were extracted with methanol at −20° C for 10 min, washed with phosphate-buffered saline (PBS), and incubated with 0.1% glycine and 0.05% Triton X–100 (octyl phenoxy polyethoxyethanol; Sigma) in PBS for 10 min. A monoclonal antibody against chicken-brain β-tubulin (Amersham, Arlington Heights, Ill., USA) diluted 1:400 in PBS containing 1% BSA served as the primary antibody. Fluorescein isothiocyanate (FITC)-conjugated anti-mouse immunoglobulin G $F(ab')_2$ fragment (Sigma) diluted 1:50, was used as the second antibody. The preparations were mounted in a medium containing 50 mM 2-amino-2-(hydroxymethyl)–1,3-propanediol (Tris) buffer, pH 9.0, 50% glycerol, 0.1% p-phenylenediamine and 1 μg/ml Hoechst 33258 (2′-(4-hydroxyphenyl)-5-(4-methyl-1-piperazinyl)-2,5′-bi-1H-benzimidazole; Sigma), and examined using a Zeiss microscope (Carl Zeiss, Oberkochen, FRG) equipped for epifluorescence illumination, using an Olympus DApo 100 UV/1.30 oil objective (Olympus Corp., Tokyo, Japan). Images were photographed on Kodak Tri-X film (Eastman-Kodak, Rochester, N.Y., USA) at ASA 400 using a Nikon UFX-II exposure system (Nikon, Nippon Kogaku K.K., Tokyo, Japan).

For centrifugation experiments, the terminal portions of cotyledons from 4-d-old seedlings were firmly wrapped in layers of paper towel moistened with water and inserted into a centrifuge tube so that centrifugal force would be directed basipetally. The material was centrifuged for 15 min at 400–1000 · *g*, the minimum force required to result in sufficient displacement of the nucleus in most small, densely cytoplasmic cells. The segments were then sliced longitudinally in half, and fixed and processed as described above.

Results

The following sequence of micrographs represents changes in the MT cytoskeleton during GC development. The sequence was assembled with reference to several criteria, including changes in the shape of the nucleus and the reappearance of nucleoli, increasing complexity of the MT array, formation of the stomatal pore, cell length and shape,

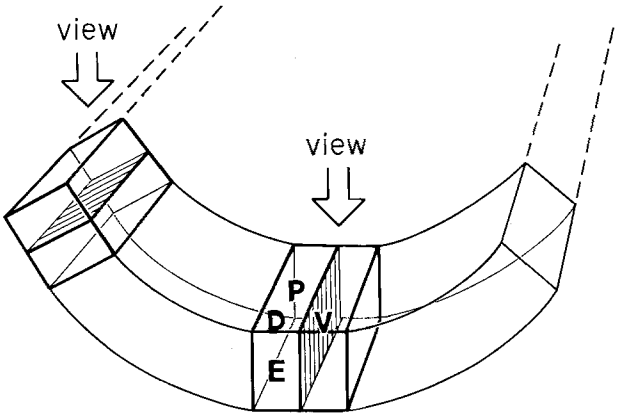

Fig. 1. Schematic diagram showing the spatial orientation of GCs of *Allium cepa* as viewed from the inside of the cotyledon. Guard-cell pairs located near the bottom of the cylindrical epidermal layer are oriented with their inner periclinal walls in face view, while cells located on the inclined sides of the cylinder are oriented obliquely in the plane of view. *D*, dorsal wall; *E*, end wall (one of two); *P*, inner periclinal wall; *V*, ventral wall (*shaded*)

seedling age, and the acropetal developmental gradient along the cotyledon. Most images are face views of the cells near their inner periclinal surface or parallel optical sections deeper into the cell (Fig. 1). In some specified cases, the cells are oriented obliquely in the plane of view. Serial optical sections are shown to provide three-dimensional information on MT distribution.

Early postcytokinetic events. The expanding phragmoplast/cell plate complex first reaches the periclinal walls in guard mother cells toward the end of cytokinesis (Fig. 2). Short MTs commonly extend from the phragmoplast toward the poles. Fusion of the cell plate with the parental walls is eventually completed along its entire circumference, thus creating two young GCs separated by an anticlinally aligned ventral wall (Figs. 3, 4). Immediately after the phragmoplast disassembles, clusters of MTs can be briefly detected in the cytoplasm some distance from the ventral wall (Fig. 3), and the cytoplasm typically shows a strong, diffuse immunofluorescence (Figs. 3, 4). In addition, prominent immunofluorescence, composed in part of short MTs, is associated with the proximal side (facing the ventral wall) of the telophase nucleus (Fig. 4). Initially the nucleus is wedge-shaped and its proximal side appears uneven, but gradually the nuclear surface becomes smooth and a nucleolus reappears.

Generation of a radial MT array. The first sign of the organization of the radial order characteristic of the GC cortex is the establishment of an incipient array of MTs, often clustered into loose aggregates, spreading from the site of the future pore in a fan-like formation along the inner periclinal wall (Figs. 5, 6). Concurrently a layer of densely aggregated MTs is seen on either side along the central strip of the ventral wall (Figs. 5b, 6b, c), which corresponds to the site of the future pore. Optical sectioning shows that the MTs avoid, rather than extend directly from, the cell edge formed

Figs. 2–14. Tubulin immunofluorescence in developing GCs of *Allium*. ×2000; scale bar in Fig. 2 = 10 μm, applies throughout

Fig. 2. Phragmoplast MTs in a cytokinetic guard mother cell in surface view. The phragmoplast is beginning to disassemble (*arrows*); note MT extensions (*arrowheads*)

Fig. 3. A pair of young GCs in surface view, immediately after cytokinesis. The GCs are separated by the anticlinal ventral wall (*arrowheads*); MTs are tilted and some criss-cross (*arrows*)

Fig. 4a, b. A pair of young GCs at a later stage after cytokinesis, showing diffuse cytoplasmic immunofluorescence. **a** Level of focus near the surface of the nucleus on left; short MTs and prominent immunofluorescence (*arrows*) are associated with the proximal side of the nucleus, *arrowheads* indicate ventral wall. **b** Nuclei stained with Hoechst 33258; *arrow* indicates a re-forming nucleolus

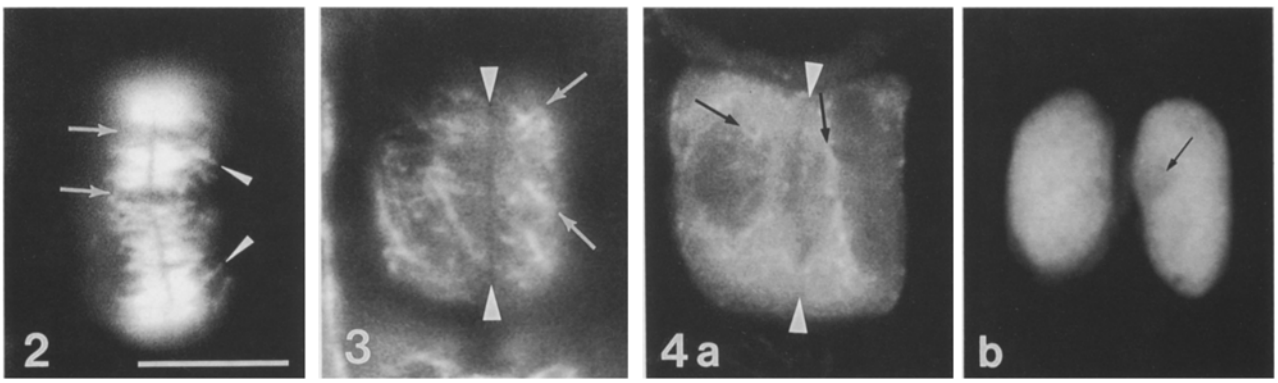

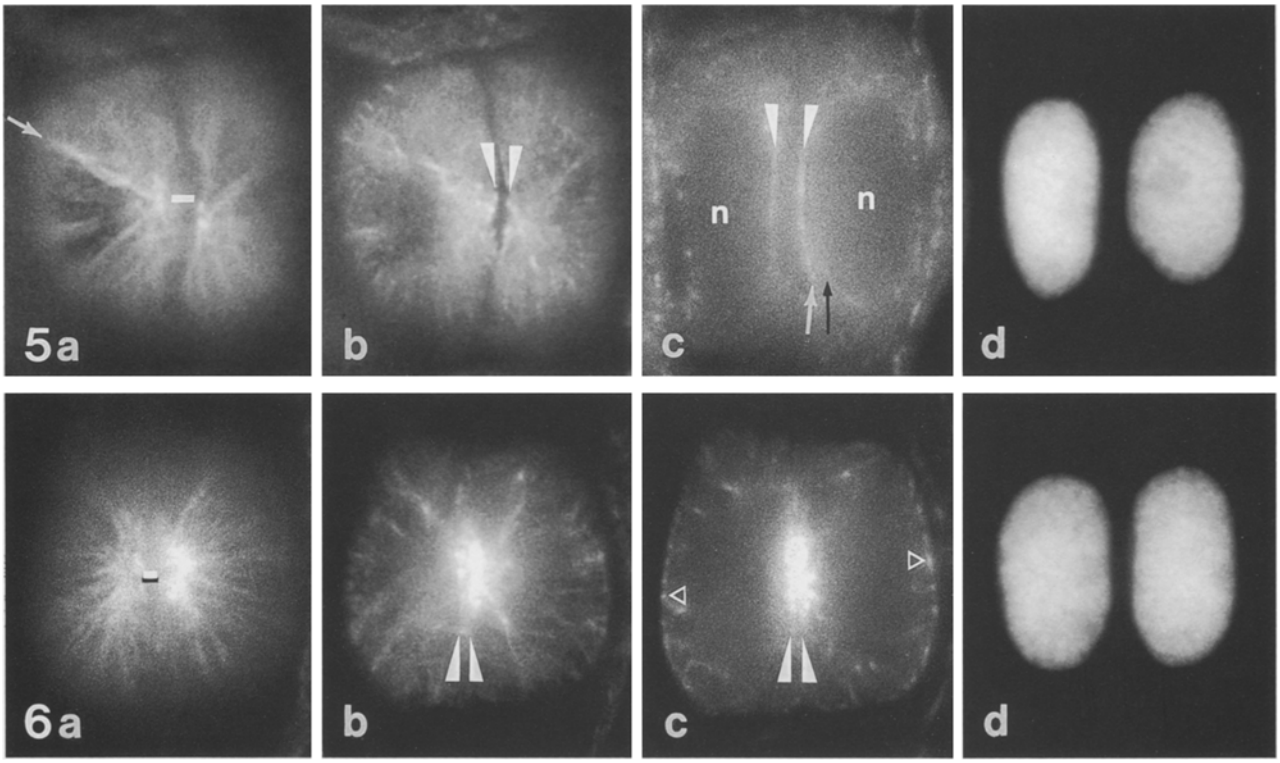

Fig. 5a–d. An incipient array of radial MTs, superimposed over a diffuse cytoplasmic immunofluorescence. **a** Focus near the periclinal wall, showing an MT aggregate (*arrow*) radiating from an MT-free gap (*bar*) at the pore site. **b** Focus slightly below the periclinal wall, showing anticlinal MTs (*arrowheads*) adjacent to the ventral wall. **c** Median optical section, showing widely separated layers of MTs (*arrowheads*); one end of the MT layer (*white arrow*) is remote from the nuclear (*n*) surface (*black arrow*), indicating that the layer is not specifically associated with the nucleus. **d** Nuclei stained with Hoechst 33258

Fig. 6a–d. A radial array of MTs, distributed evenly along the periclinal wall (**a**); *bar* indicates an MT-free gap. In optical sections at 3 μm (**b**) and 10 μm (**c**) below surface, two sets of MTs (in transverse view; *arrowheads*) are located at the pore site, one set on either side of the ventral wall. Transverse views of MTs appear also along the dorsal walls (*triangles* in **c**). **d** Nuclei stained with Hoechst 33258

by the junction of the central strip with the periclinal wall. Thus an MT-free gap appears at the edge (Figs. 5a, 6a; also Fig. 7) as an early stage in the formation of the pore, although part of this gap may consist of thickening cell wall. Focussing further down toward the median paradermal plane, the two dense layers of MTs along the ventral wall are widely separated in some cells (Fig. 5c), although this may be the result of a split in the ventral wall incurred during processing (also Fig. 8c, d). In most cells, the two dense MT layers are close together, indicating that these are adjacent to the ventral wall and are also continuous with the radial array (Fig. 6a–c). Microtubules of the radial array extend beyond the periclinal wall along the anticlinally oriented lateral, or dorsal, wall (Fig. 6c). The nucleus becomes elliptical and additional nucleoli appear. For the rest of GC development the nucleus remains in close proximity to the ventral wall.

The radial array is augmented by interpolation of additional MTs into the existing pattern (Figs. 7, 8). The array also begins to extend along the transverse, or end, walls. Again, through-focussing shows that the MTs follow a smooth curve, rather than bending sharply or terminating at wall edges, as they pass from the periclinal to the anticlinal direction. Variation in their apparent thickness and fluorescence intensity indicates that the MTs are organized into bundles (Fig. 8a). In some cells the radial pattern is nonuniform in that the most prominent MT aggregates are oriented at relatively shallow angles to the ventral wall, crossing over at the edge and then continuing down along the central strip of the ventral wall (Fig. 7). Near the mid-region of the central strip the set of MTs occasionally forms a zigzag rather than a linear arrangement (Fig. 7d), as some MTs are more remote from the ventral wall at this level. In fact,

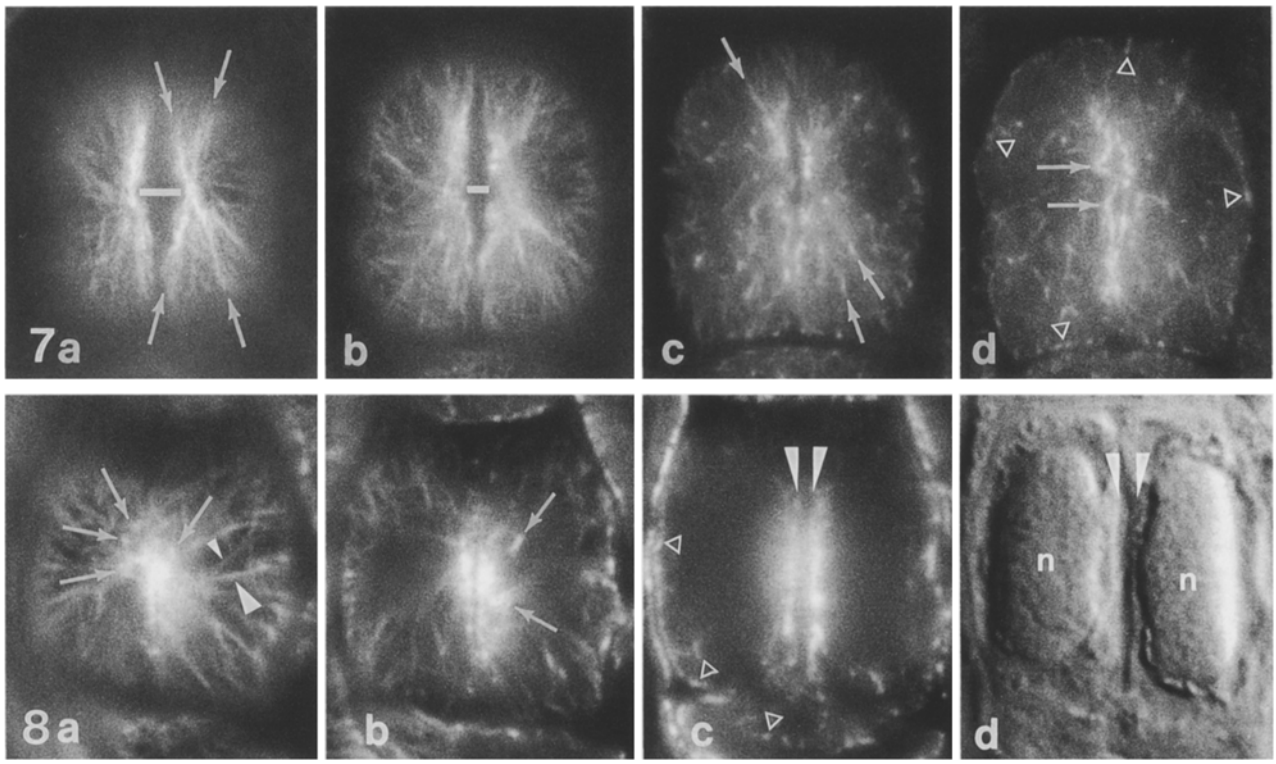

Fig. 7a–d. Serial optical sections of a pair of GCs with prominent MT aggregates (*arrows* in **a**) oriented at shallow angles to the ventral wall. An MT-free gap narrows with increasing depth of focus (*bars* in **a** and **b**). *Arrows* in **c** indicate oblique views of MTs radiating through the inner cytoplasm. A set of MTs (in transverse view) adjacent to the ventral wall near the median plane (**d**) forms a zigzag pattern (*arrows*); *triangles* indicate MTs along the dorsal and the end walls

Fig. 8a–d. Serial optical sections (**a–c**) of a pair of GCs with numerous MTs radiating through the inner cytoplasm (*arrows* in **a** and **b**). A small and a large *arrowhead* in **a** (focus slightly below the periclinal wall) show the contrast between a 'thin' MT and an MT-bundle. A linear set of MTs in transverse view is adjacent to either side of the median portion of the ventral wall (*arrowheads* in **c**); *triangles* indicate transverse views of MTs along the dorsal and the end walls. DIC view (**d**, same level as **c**) shows a partly separated ventral wall (*arrowheads*) and nuclei (*n*)

in all cells at this stage, many MTs diverge from the ventral wall and radiate past the nucleus directly through the inner cytoplasm, pointing toward various areas of the other walls (Figs. 7c, 8a, b). As in the previous stage, optical sectioning shows that the origin of these MTs can be traced to the cortex adjacent to the mid-region of the ventral wall (Fig. 8a–c). At this stage, the radial array therefore contains two components: cortical MTs, which concentrate at the mid-region of the central strip, radiate along the periclinal wall, and spread evenly along the dorsal and end walls; and cytoplasmic MTs, which radiate from the central strip through deeper portions of the cytoplasm. Because the nucleus acts as a barrier, relatively few cytoplasmic MTs are seen in the space between the far side of the nucleus and the dorsal wall cortex.

Oblique views of MTs at the pore site. The organization of MTs along the central strip of the ventral wall bordering the pore site can be examined in more detail in obliquely oriented cells in which parts of the ventral wall appear almost parallel to the plane of view (Figs. 9–11). The figures show that the orientation of these MTs is not strictly anticlinal. For example, the MTs may be arranged in sets of almost parallel elements, each set running at a different tilt toward the periclinal wall (Fig. 9). Another type consists of an array of MTs diverging in a V-shaped formation toward the periclinal wall and then spreading further along the periclinal wall (Fig. 10). Finally, the pattern may consist of sets of almost parallel MTs crossing each other at shallow angles at the pore site (Fig. 11). In most cases the MTs follow a smooth curve past the edge formed by the ventral and periclinal walls. By avoiding the edge, the MTs create a concave image (MT-free gap) at the pore site (Fig. 9b).

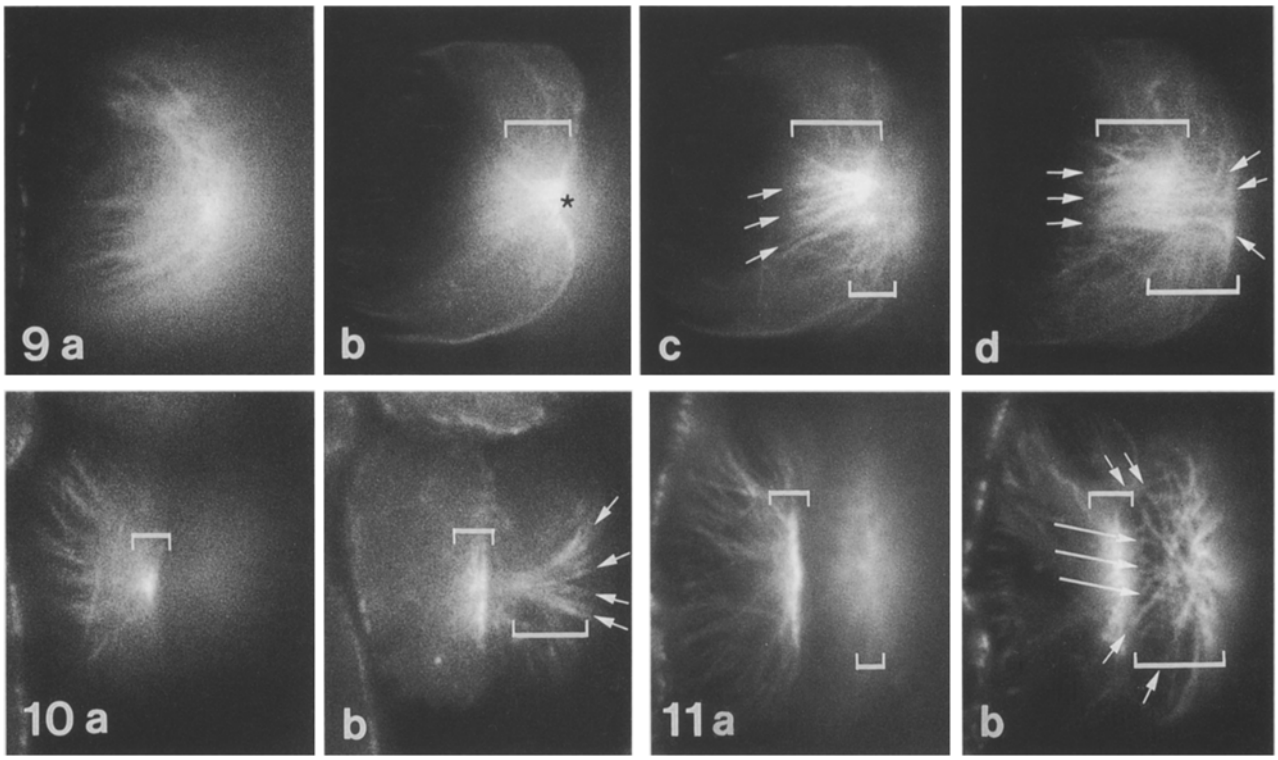

Fig. 9a–d. Serial optical sections at 0, 4, 6, and 8 μm through a pair of GCs oriented in almost side-view. Upper and lower brackets indicate the pore site corresponding to the upper and lower cells, respectively. *Asterisk* in **b** indicates a depression at the pore site. *Arrows* pointing to the right in **c** and **d** show the orientation of sets of almost parallel MTs; note that the sets corresponding to the upper cell change their orientation between **c** and **d**, and that MTs in the lower cell spread out toward the periclinal wall (left-pointing *arrows* in **d**)

Fig. 10a, b. A pair of GCs oriented in an oblique view. Notation by brackets as in Fig. 9. **a** Oblique view of the radial array along the periclinal wall. **b** Transverse view of the pore site of the upper cell and face view of the pore site of the lower cell; *arrows* indicate spreading MTs in a V-shaped formation

Fig. 11a, b. A pair of GCs oriented in oblique view, showing sets of MTs (*arrows* in **b**) crossing each other at shallow angles at the pore site. Notation by brackets as in Fig. 9. **a** Focus on upper cell. **b** Face view of the pore site of the lower cell

Cell expansion and shaping. As the GCs expand they gradually assume a kidney-shape (Figs. 12, 13). The junctions between the dorsal and end walls round off, and the end portions of the inner periclinal wall bulge above its central portion. Nevertheless the spatial organization of the radial array of MTs is maintained, with modification in detail. Compared with earlier stages, cortical MTs now predominate while the frequency of cytoplasmic MTs diminishes. The MTs also generally appear to be arranged in relatively thick bundles. Those adjacent to the pore frequently cross over, like spokes on a bicycle wheel (Figs. 12b, 13b), while those located at the bulging ends of the periclinal wall are almost parallel (Fig. 13a). The MT-free gap at the pore site enlarges both laterally and down toward the median plane. At this stage, MTs also extend from the mid-region of the central strip along the ventral wall toward the end walls, that is, parallel to the periclinal wall (Figs. 12c, 13d). Microtubules running along the dorsal and end walls now appear as a distinct layer, although in about half of the cells at this stage the layer does not spread all the way to the junctions of the end walls with the ventral wall (Fig. 13d). Cell expansion is accompanied by vacuolation, seen as regions devoid of diffuse cytoplasmic immunofluorescence (Fig. 13e) and visible also in differential interference contrast (DIC) images (not shown).

Cell expansion proceeds until the ventral walls of the two GCs separate along the entire central strip and the cells become flexed into a rounded shape, thus forming a complete stomatal pore (Fig. 14). Most MTs are now cortical. A large, lobed vacuole occupies most of the cell interior (seen in DIC, not shown here; see also Palevitz et al. 1981), leaving a thin layer of cytoplasm to-

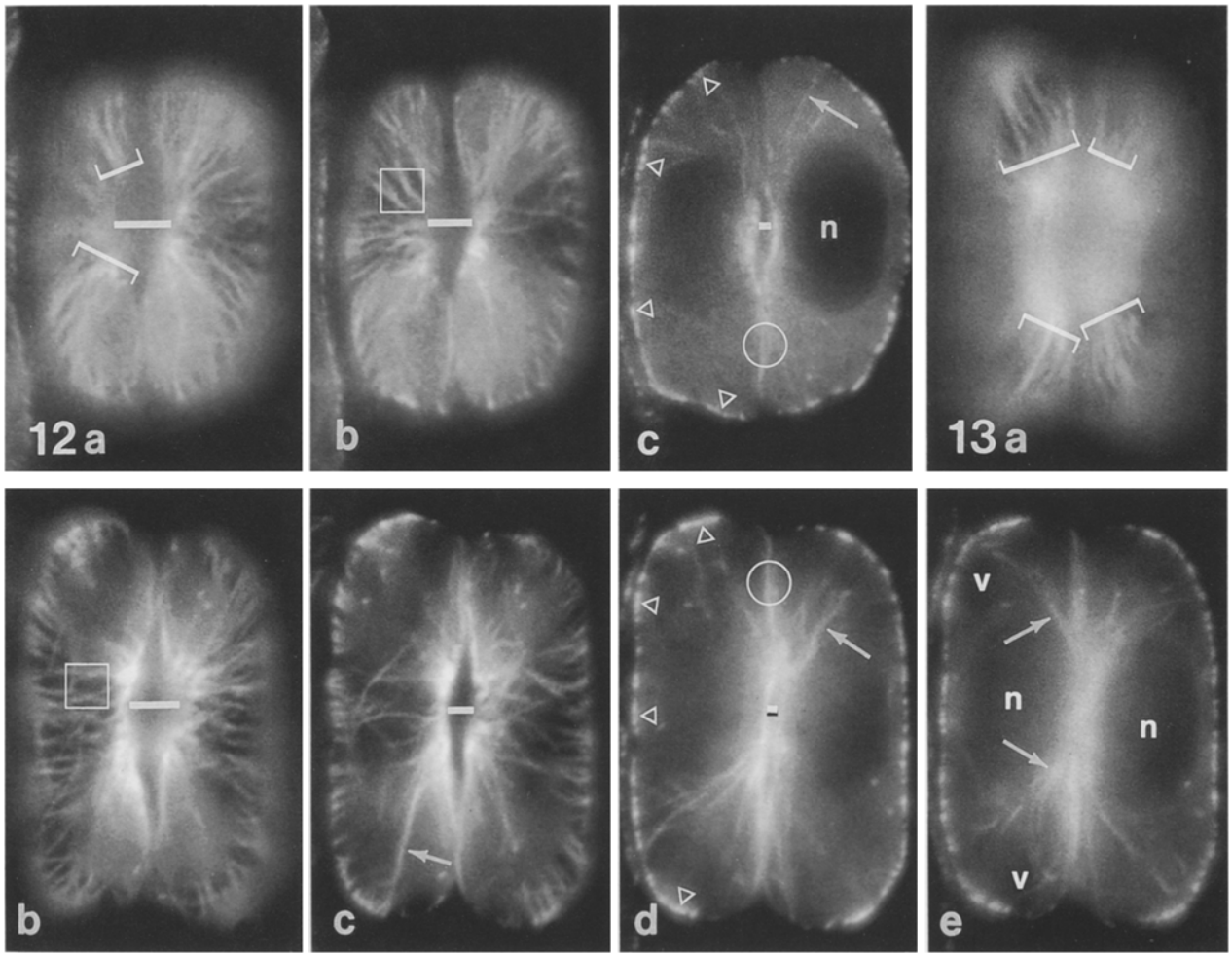

Fig. 12a–c. Serial optical sections through a partially expanded pair of GCs. *Brackets* in **a** indicate protruding cell ends. A *square* in **b** shows MT bundles that criss-cross near the pore site. The width of the MT-free gap (*bars* in **a–c**) at the pore site decreases toward the median portion of the cell (**c**); *triangles* show transverse views of MTs lining the dorsal and the end walls, periclinally oriented MTs (*circle*) extend from the pore site toward the end walls, and some MTs (*arrow*) radiate past the nucleus (*n*) but do not specifically associate with it

Fig. 13a–e. Serial optical sections through an expanding pair of GCs in which distinct vacuoles (*v*) have begun to appear. Other notation as in Fig. 12. Note that MTs along the end wall do not extend completely to the junction with the ventral wall (*triangles* in **d**); *arrows* in **c–e** indicate remaining prominent MT bundles in the cytoplasm

gether with any remaining MTs and a diffuse immunofluorescence lining the walls and the now spherical nucleus (Fig. 14d). The fluorescent signal seen around the nucleus therefore probably represents a passive association. The arrangement of cortical MTs is similar to that seen earlier, except that the layer of MTs along the end walls again spreads all the way to the junctions with the ventral wall (Fig. 14d). Also, the density of the MT layer is slightly reduced at the central portion of the dorsal wall, which may undergo more extensive elongation relative to the end portions. Compared to the earlier developmental stages (Figs. 7, 12, 13), however, the overall apparent density of cortical MTs seems to be maintained, if not increased, although the surface area of the GC increases approximately threefold (data not shown).

Centrifugation studies. Because of the close proximity of the nucleus to the ventral wall, and because the perinuclear region has been implicated in MT nucleation in some cells (e.g. Clayton et al. 1985; Wick 1985), we centrifuged the cotyledons before processing for immunofluorescence microscopy in order to displace the nucleus (Figs. 15–18). In very young GCs, which typically contain short, randomly oriented MTs as well as diffuse cytoplasmic

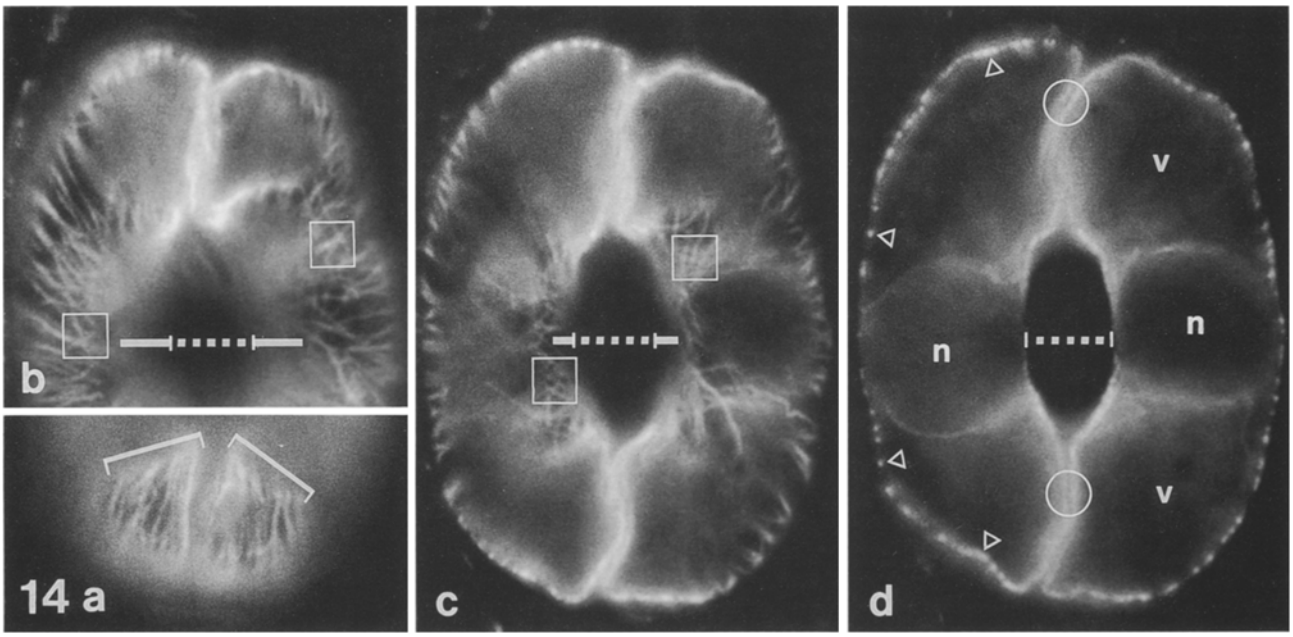

Fig. 14a–d. Serial optical sections of an expanded, mature pair of GCs. *Brackets* in **a** indicate nearly parallel MTs in the bulging cell ends; *bars* in **b** and **c** indicate the width of the MT-free gap, which now also includes the space between the separated ventral walls as seen at the median paradermal plane (*dots* in **c**). A frequent criss-crossing of MTs occurs along the periclinal wall as well as deeper at the pore site (*squares* in **b** and **c**). **d** Median optical section; a large vacuole (*v*) occupies the cell interior, and the cells border a stomatal pore. Note that the density of MTs along the dorsal wall (*triangles*) is relatively low at its central portion, and that MTs along the end wall now extend to the junction with the ventral wall. *Circles* indicate periclinally oriented MTs

fluorescence but no radial array, MTs trail behind the displaced nucleus and a prominent fluorescent signal remains attached to its irregular proximal side, but few or no MTs are specifically associated with the ventral wall (Fig. 15). In the somewhat older GC pair in Fig. 16, the proximal side of the nucleus is now almost smooth and relatively few MTs trail behind the displaced nucleus. Although some MTs appear to associate with the ventral wall, there is no sign of a radial array yet. In still older GCs (Fig. 17), perinuclear and randomly oriented cytoplasmic MTs are absent. Instead, a distinct planar set of highly aggregated MTs remains attached to the cortex on either side of the central portion of the ventral wall. Even though the nucleus has been displaced, a centrally located radial pattern is apparent. This situation persists for the rest of GC development (Fig. 18).

Kinetics of MT-array development. In order to assess the time needed for the changes in MT organization documented above, we scored the frequencies of individual developmental stages in the cotyledons of 4-, 5-, and 6-d-old seedlings and compared them to the frequencies of the mitotic phases in nearby guard mother cells (Table 1). For this purpose the developmental pathway was arbitrarily divided into four stages, defined as 'postcytokinetic' (as in Figs. 3, 4), 'incipient' (as in Figs. 5, 6), 'established' (as in Figs. 7, 8, 12), and 'mature' (as in Figs. 13, 14). We emphasize, however, that GC development is a continuous process.

By day 4, asymmetric divisions in protodermal cells have almost ceased, mature GC pairs comprise 5.9% of the total cell population, and all non-stomatal epidermal cells together with interphase guard mother cells represent a total of 85.8% (Table 1). The sum of guard mother cells in mitosis (mitotic index) remains at 3.0% and 3.2% on days 4 and 5, but falls to a negligible value by day 6. By this time, the proportion of non-stomatal epidermal cells has been significantly (probability level 0.05) reduced to 65.8%, as all the guard mother cells have departed into the developmental pathway. At the same time, the proportion of cells in the 'mature' stage has significantly increased to a total of 32.5%. Since mitosis has been completed and only 1.4% cells remain to leave the 'established' stage, the wave of mitoses and GC differentiation has been largely completed in the two days, giving a final ratio of almost two epidermal cells to one GC pair.

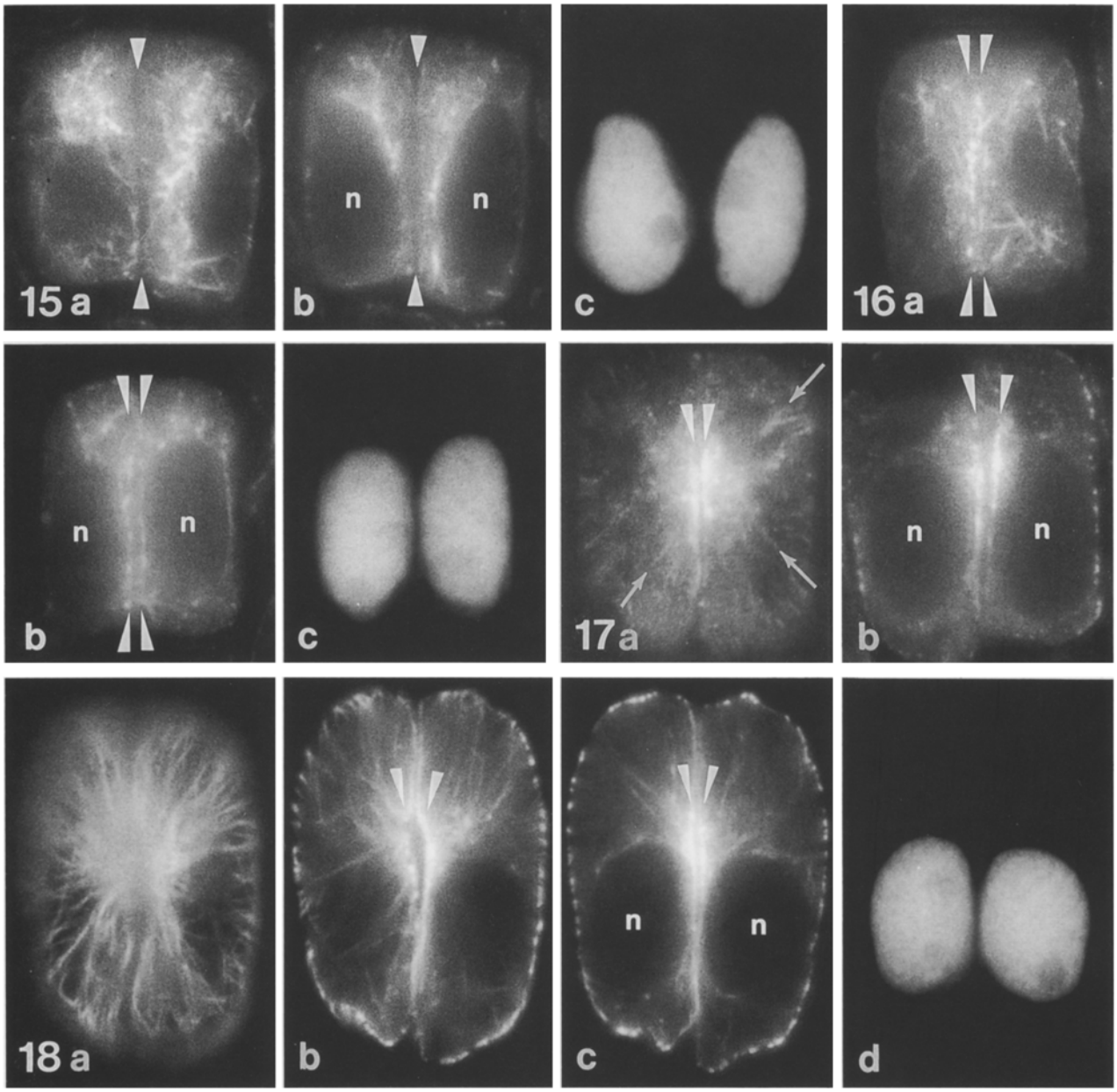

Figs. 15–18. Tubulin immunofluorescence in *Allium* GCs after centrifugation. The direction of centrifugal force is toward the bottom of the page. × 2000

Fig. 15a–c. A young GC pair. **a** Focus near the upper surface of the nucleus; **b** median optical section. Numerous short MTs are distributed throughout the cytoplasm of the two cells separated by the ventral wall (*arrowheads*). Short MTs or prominent fluorescence is associated with the proximal side of the displaced nuclei (*n*), and some MTs trail behind the nuclei. **c** Nuclei stained with Hoechst 33258; note irregular shape

Fig. 16a–c. A slightly older GC pair, separated by only one intervening epidermal cell from the GC pair in Fig. 15. Optical sections as in Fig. 15. The perinuclear fluorescence is less distinct, although some MTs are still trailing the displaced nucleus (*n*). A row of MTs in transverse section (*arrowheads*) appears on each side of the ventral wall. **c** Nuclei stained with Hoechst 33258; note their more regular shape

Fig. 17a, b. An incipient radial array of MTs (*arrows*). **a** Focus slightly below cell surface; **b** median optical section. A distinct set of densely aggregated MTs in transverse section is located centrally on either side of the ventral wall (*arrowheads*), away from the displaced nucleus (*n*); note paucity of fluorescence around the nucleus

Fig. 18a–d. A partially expanded GC pair with an established radial array of MTs. **a** Focus at cell surface; **b** focus near the upper surface of the nucleus; **c** median optical section. Distinct sets of densely aggregated MTs (*arrowheads*) remain located centrally at the ventral wall while the nucleus (*n*) has been displaced. **d** Nuclei stained with Hoechst 33258

Table 1. Frequency distribution (% of total cell population) of developmental stages in guard cells and mitotic phases in guard mother cells in epidermal layers of 4-, 5-, and 6-d-old *Allium cepa* seedlings. Values are means of 100–300 cells in each of the epidermal layers evaluated (*n*). Any two or more values followed by the same letter (s–z) are not statistically different at the 0.05 probability level (LSD multiple range test). Standard errors are in parentheses

Age (d)	*n*	Epidermal cells[a]	Mitotic guard mother cells				Developing guard cell pairs			
			Pro-phase[b]	Meta-phase[c]	Ana-phase	Cytoki-nesis[d]	Post-cytok.	Inci-pient	Estab-lished	Mature[e]
4	11	85.8^{s} (1.7)	1.4^{yz} (0.4)	0.2^{z} (0.1)	0.1^{z} (0.1)	1.3^{yz} (0.6)	0.2^{z} (0.1)	1.7^{yz} (0.7)	3.4^{yz} (0.9)	5.9^{xy} (1.0)
5	9	72.7^{t} (2.3)	1.4^{yz} (0.3)	0.7^{yz} (0.3)	0.4^{z} (0.2)	0.7^{yz} (0.3)	0.6^{z} (0.4)	2.5^{yz} (0.6)	9.5^{wx} (1.1)	11.6^{w} (2.0)
6	4	65.8^{tu} (3.5)	0	0.2^{yz} (0.2)	0	0	0	0	1.4^{yz} (0.6)	32.5^{v} (2.9)

[a] Non-stomatal cells and interphase guard mother cells
[b] Guard mother cells with preprophase band of microtubules
[c] Includes prometaphase
[d] Guard mother cells with phragmoplast microtubules
[e] Includes mature stomata (4.6% on day 4) that had developed before the main wave of mitoses and guard-cell differentiation

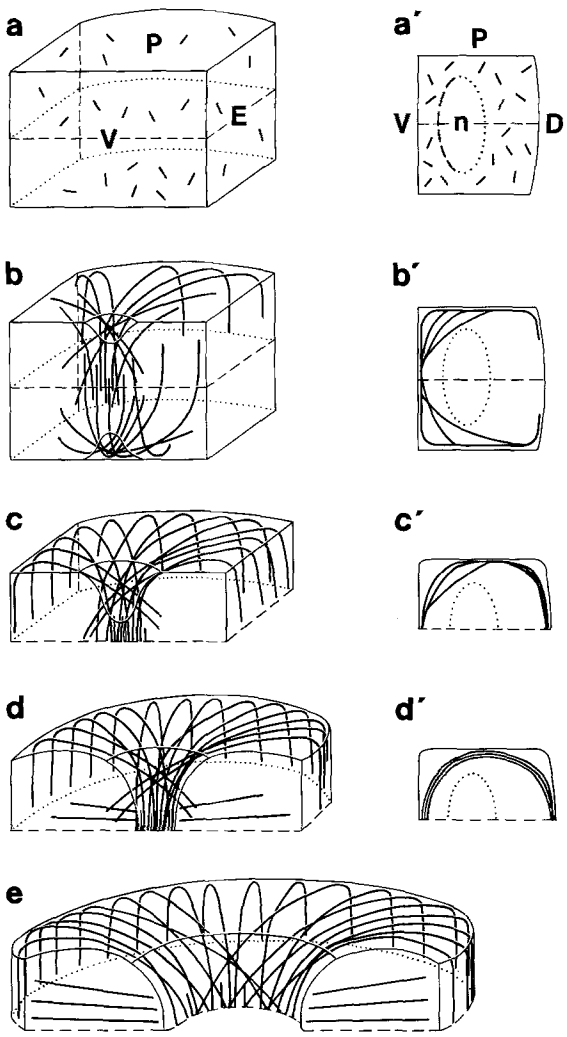

Analysis of individual developmental stages shows that the value for the 'established' stage increases significantly on day 5, probably reflecting a peak of activity in the two-day wave of mitoses and GC differentiation. Values for the 'postcytokinetic' and 'incipient' stages, however, do not change significantly between days 4 and 5, and the same applies also to the mitotic phases. Although the differences are not significant at the 0.05 probability level, the relatively low values for the 'postcytokinetic' stage are similar to those for metaphase or anaphase, while the distinctly higher

Fig. 19a–e. Schematic diagrams showing the development of a radial array of MTs in a GC oriented with the ventral wall in face view (**a–e**) and in corresponding transverse sections (parallel to the end walls) through the central portion of the cell (**a'–d'**). In **c, c'–e** only half the array is presented for the sake of simplicity. *D* dorsal wall, *E* end wall, *P* periclinal wall, *V* ventral wall, *n* nucleus. **a, a'** Early postcytokinetic stage with diffuse cytoplasmic immunofluorescence and a fluorescent signal at the proximal side of the nucleus. **b, b'** An incipient array of MTs originating from the mid-region of the central strip of the ventral wall and radiating along the periclinal wall as well as directly through the inner cytoplasm. **c, c'** An established radial array of MTs extending distally along the dorsal and end walls; MTs become consolidated into bundles. **d, d'** An expanding cell in which the edges between the dorsal and end walls are rounded. The MTs have retracted from the edge where the central strip of the ventral wall joins the periclinal wall, thus creating a space that extends to the median periclinal plane. Periclinally oriented MTs extend from the pore site toward the end walls. **e** An expanded, mature GC, flexed into a rounded shape and forming a distinct stomatal pore

values for the 'incipient' stage are more similar to those for prophase or cytokinesis.

Discussion

The immunofluorescence images shown here provide a much more complete, as well as a somewhat different, view of the MT cytoskeleton in the guard cell than has previously been available. The chief finding of this work is that the radial array initially contains cortical as well as cytoplasmic MTs, and that both originate from a planar MT-organizing zone in the cortical cytoplasm adjacent to the central portion of the ventral wall. Contrary to previous reports, MTs extending from the zone arc past, rather than being initiated at, cell edges. Moreover, there is no evidence for an involvement of perinuclear MTs in the generation of the radial array.

Early postcytokinetic events. The short MTs remaining in the cytoplasm immediately after cytokinesis are more likely to be related to the phragmoplast extensions noted late in cytokinesis rather than to the radial array, since their location and orientation do not correspond to the geometry of the future array and they are ephemeral. In fact the entire 'postcytokinetic' stage is relatively brief, its duration being similar to that of anaphase or metaphase (see below).

Although it has been suggested that interphase cortical MTs originate in the perinuclear region in root tip cells (Clayton et al. 1985; Wick 1985), it is unlikely that the GC nucleus provides MTs for the radial array, despite its location deceptively close to the ventral wall. The immunofluorescent signal at the proximal side of the nucleus is probably associated with reformation of the nuclear envelope since this side is the last to become smooth in outline. The fluorescence may briefly persist beyond telophase due to the high concentration of free tubulin presumably released by the disassembly of the phragmoplast. Based on many observations, the occurrence of cells that show both the perinuclear signal and signs of initiation of a radial array is extremely rare. This indicates that such a stage either does not occur in all cells or it is very short, perhaps on the order of a few minutes. As shown by the centrifugation experiments, the perinuclear signal is absent most of the time during which the radial array is generated. When the nucleus is displaced, the radial array can clearly be seen to arise from the cortex adjacent to the ventral wall.

Origin and organization of the radial MT array. As with the perinuclear MTs, our micrographs are also inconsistent with an origin of the radial array at cell edges. Optical sections show that many MTs criss-cross as they pass the edge between the ventral and the periclinal walls, but they do not terminate there. Relatively bright fluorescent spots appear when focussing through this region, but these correspond to locations where MTs overlap or where they are seen at oblique angles. Conceivably, an ultrathin section through such a region would appear to contain clusters of converging or terminating MTs of different orientations, similar to those seen previously in electron micrographs (Galatis 1980; Galatis et al. 1983). Thus the MTs, or more likely bundles, are continuous, bending smoothly past the edge and then extending along the periclinal wall (see also Apostolakos and Galatis 1985), indicating that the edge itself is not involved in significant MT-initiation activity. The MTs also bend smoothly past the edges where the periclinal wall joins the dorsal and end walls. In addition, many MTs originating at the mid-region of the central strip radiate directly through the inner cytoplasm, avoiding the edge with the periclinal wall completely. Similarly placed MTs can be seen also in electron micrographs of GCs in *Adiantum* (Galatis et al. 1983) and *Azolla* (Busby and Gunning 1984), but a full appreciation for the number and extent of such MTs is only seen with the immunofluorescence images shown here.

Since the MTs aggregate along the mid-region of the central strip of the ventral wall from the inception of the radial array, and this region acts as a focal site for both cortical and cytoplasmic MTs, it appears to function as a planar MT-organizing zone (see also Schnepf 1984). Furthermore, in separate experiments we have found that MTs along this zone are the last to disassemble during cold- or colchicine-induced depolymerization, and conversely, the first to reassemble during recovery (Marc et al. 1989).

Although we have concentrated our observations on the inner half of the GC, views of cells that have been accidentally sliced open during preparation indicate that the spatial organization of MTs in the inner and outer halves represent near mirror-images (see diagram in Fig. 19; also Cleary and Hardham 1989). We therefore presume that MTs originating at the MT-organizing zone grow distally in either direction toward the periclinal walls. At the distal ends of each half-array, that is along the dorsal and the end walls, the two sets of MTs presumably meet or interdigitate. On either side of the ventral wall, the complete array

in one GC also represents a near mirror-image of that in the adjacent GC.

It is conceivable that cortical MTs (or bundles) growing from the zone conform to the geometry of the cell by bending into an arc upon contact with the cortex or plasmalemma at the periclinal wall, thus avoiding the extreme edge, and then continue along the periclinal wall while maintaining their original course (Fig. 19). Since the MT-organizing zone is located centrally, MTs originating at any point and diverging in any direction will inevitably generate an overall radial pattern. Depending on their point of origin and the angle of tilt, some MTs therefore cross each other, this occurring most frequently in regions facing the zone. Such criss-crossing, together with progressive MT bundling and incorporation of cytoplasmic MTs, presumably leads to increasing rigidity of the MT layer and consequently straightening of its curvature at the cell edge (Fig. 19b′–d′). The MT layer could therefore retract from the original cell edge (see also Galatis 1988), particularly at the pore site, thus enlarging the MT-free gap. It is unknown, however, what proportion of the gap is occupied by the developing pore itself, by the thickness of the cell wall, and possibly also by cytoplasm, depending on how closely the cell wall follows the retracting MT layer. The geometry of the gap may be further complicated by lateral expansion and rounding of the cell.

As shown by the variation in thickness and fluorescence intensity of MT images during GC development, individual MTs become increasingly consolidated into relatively thick bundles that probably span half of the cell circumference. That the changes in fluorescence properties represent enhanced MT bundling is supported by observation of clusters of parallel MTs in *Allium* GCs in the electron microscope (Doohan and Palevitz 1980). Similar bundles have been seen as well in other plants and cell types (Gunning and Hardham 1982; Quader et al. 1986). Formation of such bundles presumably involves unique MT-associated, or 'bundling', proteins (Cyr and Palevitz 1989). At this stage the frequency of cytoplasmic MTs decreases and cortical MTs predominate. It is unclear whether this shift involves depolymerization and reassembly, or simply relocation of existing MTs. Either way, it represents an increase in the affinity of MTs for the cortex or plasmalemma, which may be related to the MT-bundling process and involve the same type of proteins. Cross bridges between MTs and the plasmalemma occur in many cell types (Hardham and Gunning 1978; Galatis and Mitrakos 1980; Gunning and Hardham 1982; Palevitz 1982), and in *Allium* GCs they apparently are not affected by the centrifugal forces used here, or by the process of protoplast formation (Doohan and Palevitz 1980).

Kinetics of MT array development. As indicated by the results in Table 1, the generation of the radial array is a dynamic process. The sum of percentages of GCs progressing through the first three developmental stages on day 4 (5.3%) is almost sufficient to account for the significant increment in the 'mature' stage between days 4 and 5 (5.7%), indicating that the entire progression can be accomplished within one day. A similar calculation applied to the situation between days 5 and 6 shows, however, that the sum of the first three stages on day 5 (12.6%) is roughly only half of the significant increment in the 'mature' stage (20.9%). The rest of the increment is presumably the result of a continuous inflow of cells that have passed through the mitotic compartment, progressed through the developmental stages, and entered the 'mature' stage. Therefore the progression of the GC through the first three developmental stages is more likely accomplished within about half a day.

The duration of individual stages can be estimated indirectly by assuming that the sequence from prophase to the 'incipient' stage occurs asynchronously between days 4 and 5 and therefore the frequency of cells in a particular mitotic phase or developmental stage is proportional to the time spent in that phase or stage. Observations of living *Allium* cells in DIC have shown that anaphase in the guard mother cell lasts 10–20 min (Hepler and Palevitz 1986), and cytokinesis 30–40 min (Palevitz 1986). By using 15 min as the average duration of anaphase (average frequency 0.3%), the 'postcytokinetic' stage (average frequency 0.4%) would therefore occupy an equivalent time (20 min), while the 'incipient' stage would last approx. 6–8 times longer (1–2 h) and the 'established' stage 11–32 times longer (3–8 h). Thus the generation of the 'incipient' stage of the radial MT array takes about 1.5–3 times longer than cytokinesis, while most of the time of GC development is occupied by the augmentation and consolidation of the radial array and by the cell expansion and maturation stages.

It seems plausible that the 20-min lag after cytokinesis and before the beginning of generation of the radial array is occupied by the establishment of the necessary MT-organizing centers at the ventral wall. By taking an MT growth rate of 4 μm/min (Schulze and Kirschner 1987), it can be calcu-

lated that it would take less than 5 min for a growing MT to span half of the cell circumference. Therefore the limiting factor in accomplishing the relatively longer 'incipient' stage is more likely to be the time needed to generate the necessary number of MTs. This may be related to the number of available nucleating sites or to the concentration of tubulin, which is known to directly influence the number of MTs nucleated by a centrosome (Mitchison and Kirschner 1984). The duration of the much longer 'established' stage could be accounted for if, besides generating more MTs, it involves additional events such as the apparent shift from cytoplasmic to predominantly cortical MTs and their bundling and bridging to the plasma membrane. Thus the immunofluorescent images, which provide the basis for the above estimates of the developmental kinetics, should be viewed as the end product of a complex process involving not only the initiation and growth of MTs, but also their dynamics and various forms of stabilization and chemical modification (e.g. Kirschner and Mitchison 1986; Schulze and Kirschner 1987).

We thank Dr. Gary Kochert for help with statistics, Dr. Richard J. Cyr for providing valuable suggestions during the preparation of this manuscript, and Ms. Elizabeth Bruce for printing the figures. This research was supported by funds from the University of Georgia Center for Plant Cell and Molecular Biology, and National Science Foundation grants DCB-8703292 to B.A.P. and DCB-8803286 to B.A.P. and J.M.

References

Apostolakos, P., Galatis, B. (1985) Studies on the development of the air pores and air chambers of *Marchantia paleacea*. II. Ultrastructure of the initial aperture formation with particular reference to cortical microtubule organizing centres. Can. J. Bot. **63**, 744–756

Busby, C.H., Gunning, B.E.S. (1984) Microtubules and morphogenesis in stomata of the water fern *Azolla:* an unusual mode of guard cell and pore development. Protoplasma **122**, 108–119

Clayton, L., Black, C.M., Lloyd, C.W. (1985) Microtubule nucleating sites in higher plant cells identified by an auto-antibody against pericentriolar material. J. Cell Biol. **101**, 319–324

Cleary, A.L., Hardham, A.R. (1989) Microtubule organization during development of stomatal complexes in *Lolium rigidum*. Protoplasma (in press)

Cyr, R.J., Palevitz, B.A. (1989) Microtubule-binding proteins from carrot. I. Initial characterization and microtubule bundling. Planta **177**, 245–260

Doohan, M.E., Palevitz, B.A. (1980) Microtubules and coated vesicles in guard-cell protoplasts of *Allium cepa* L. Planta **149**, 389–401

Galatis, B. (1980) Microtubules and guard-cell morphogenesis in *Zea mays* L. J. Cell Sci. **45**, 211–244

Galatis, B. (1982) The organization of microtubules in guard cell mother cells of *Zea mays*. Can. J. Bot. **60**, 1148–1166

Galatis, B. (1988) Microtubules and epithem-cell morphogenesis in hydathodes of *Pilea cadierei*. Planta **176**, 287–297

Galatis, B., Mitrakos, K. (1980) The ultrastructural cytology of the differentiating guard cells of *Vigna sinensis*. Am. J. Bot. **67**, 1243–1261

Galatis, B., Apostolakos, P., Katsaros, C. (1983) Microtubules and their organizing centres in differentiating guard cells of *Adiantum capillus veneris*. Protoplasma **115**, 176–192

Giddings, T.H., Jr., Staehelin, L.A. (1988) Spatial relationship between microtubules and plasma-membrane rosettes during the deposition of primary wall microfibrils in *Closterium* sp. Planta **173**, 22–30

Gunning, B.E.S., Hardham, A.R. (1982) Microtubules. Annu. Rev. Plant Physiol. **33**, 651–698

Hardham, A.R., Gunning, B.E.S. (1978) Structure of cortical microtubule arrays in plant cells. J. Cell Biol. **77**, 14–34

Hepler, P.K. (1981) Morphogenesis of tracheary elements and guard cells. In: Cytomorphogenesis in plants, pp. 327–347, Kiermayer, O., ed. Springer, Wien New York

Hepler, P.K., Palevitz, B.A. (1986) Metabolic inhibitors block anaphase A in vivo. J. Cell Biol. **102**, 1995–2005

Kaufman, P.B., Petering, L.B., Yocum, C.S., Baic, D. (1970) Ultrastructural studies on stomata development in internodes of *Avena sativa*. Am. J. Bot. **57**, 33–49

Kirschner, M., Mitchison, T. (1986) Beyond self-assembly: from microtubules to morphogenesis. Cell **45**, 329–342

Marc, J., Hackett, P.W. (1989) A new method for immunofluorescent localization of microtubules in surface cell layers: application to the shoot apical meristem of *Hedera*. Protoplasma **148**, 70–79

Marc, J., Mineyuki, Y., Palevitz, B.A. (1989) A planar microtubule-organizing zone in guard cells of *Allium:* experimental depolymerization and reassembly of microtubules. Planta **179**, 530–540

Mishkind, M., Palevitz, B.A., Raikhel, N.V. (1981) Cell wall architecture: normal development and environmental modification of guard cells of the Cyperaceae and related species. Plant Cell Environ. **4**, 319–328

Mitchison, T., Kirschner, M. (1984) Microtubule assembly nucleated by isolated centrosomes. Nature **312**, 232–237

Palevitz, B.A. (1981 a) The structure and development of stomatal cells. In: Stomatal physiology, pp. 1–23, Jarvis, P.E., Mansfield, T.A., eds. Cambridge University Press, Cambridge, UK

Palevitz, B.A. (1981 b) Microtubules and possible microtubule nucleation centers in the cortex of stomatal cells as visualized by high voltage electron microscopy. Protoplasma **107**, 115–125

Palevitz, B.A. (1982) The stomatal complex as a model of cytoskeletal participation in cell differentiation. In: The cytoskeleton in plant growth and development, pp. 345–376, Lloyd, C.W., ed. Academic Press, London

Palevitz, B.A. (1986) Division plane determination in guard mother cells of *Allium:* video time-lapse analysis of nuclear movements and phragmoplast rotation in the cortex. Dev. Biol. **117**, 644–654

Palevitz, B.A., Hepler, P.K. (1976) Cellulose microfibril orientation and cell shaping in developing guard cells of *Allium:* the role of microtubules and ion accumulation. Planta **132**, 71–93

Palevitz, B.A., Mullinax, J.B. (1989) Developmental changes in the arrangement of cortical microtubules in stomatal cells of oat (*Avena sativa* L.). Cell Motil. Cytoskeleton **13**, 170–180

Palevitz, B.A., O'Kane, D.J., Kobres, R.E., Raikhel, N.V. (1981) Vacuole movements and changes in morphology in

differentiating cells as revealed by epifluorescence, video and electron microscopy. Protoplasma **109**, 23–55

Quader, H., Deichgraber, G., Schnepf, E. (1986) The cytoskeleton of *Cobaea* seed hairs: patterning during cell-wall differentiation. Planta **168**, 1–10

Raschke, K. (1979) Movements of stomata. In: Encyclopedia of plant physiology, N.S., vol. 7. Physiology of movements, pp. 385–441, Haupt, W., Feinleib, M.E., eds. Springer, Berlin Heidelberg New York

Sack, F.D., Paolillo, D.J., Jr. (1983) Protoplasmic changes during stomatal development in *Funaria*. Can. J. Bot. **61**, 2515–2526

Schnepf, E. (1984) Pre- and postmitotic reorientation of microtubule arrays in young *Sphagnum* leaflets: transitional stages and initiation sites. Protoplasma **120**, 100–112

Schulze, E., Kirschner, M. (1987) Dynamic and stable populations of microtubules in cells. J. Cell Biol. **104**, 277–288

Singh, A.P., Srivastava, L.M. (1973) The fine structure of pea stomata. Protoplasma **76**, 61–82

Srivastava, L.M., Singh, A.P. (1972) Stomatal structure in corn leaves. J. Ultrastruct. Res. **39**, 345–363

Wick, S.M. (1985) The higher plant mitotic apparatus: redistribution of microtubules, calmodulin and microtubule initiation material during its establishment. Cytobios **43**, 285–294

Received 11 May; accepted 18 July 1989